Journal Name

COMMUNICATION

Structural, spectroscopic and electronic properties of a family of bi-octahedral mixed-valence Ru_2^{5+} complexes with a bridging 2,5-di(2-pyridyl)pyrrolide ligand

Received 00th January 20xx,
Accepted 00th January 20xx

DOI: 10.1039/x0xx00000x

www.rsc.org/

Shi-Rui Kang,[a] Zi-Qin Zhou,[b] Chang-Feng Xiong,[a] Bin Liu,*[b] John E. McGrady,*[c] Mohammed Obies,[c,d] Chao Liu,[a] Zheng-Hao Zhang,[a] Piao He,[a] Xiao-Yi Yi*[a]

A family of Ru_2 dimers, $[Ru_2(\mu\text{-}\kappa_2N,N':\kappa_2N',N''\text{-dpp})_2(\mu\text{-X})(X)_2]^{q+}$ (X = Cl, Br, q = 0 and X = I, q = 1) is synthesized from a $[Ru_2(OAc)_4Cl]$ paddlewheel starting material. The neutral products are mixed-valence Ru_2^{5+} dimers with a Ru-Ru bond order of 0.5, while the cationic iodide is a Ru_2^{5+} dimer with formal bond order of 1.0. The Ru-Ru distance is strikingly independent of the identity of the halide and the oxidation state of ruthenium, most likely a consequence of the small bridging nitrogen which constrains the geometry. The spectroscopic properties (EPR, UV/Vis) of the Br complex are consistent with a large σ-σ* splitting in $Ru_2(\mu\text{-}\kappa_2N,N':\kappa_2N',N''\text{-dpp})_2(\mu\text{-Br})(Br)_2$].

Bimetallic units with direct covalent bonds between the metals have long held the interest of chemists and physicists, primarily due to the remarkable variations in structure, spectroscopy and magnetism.[1] More recently, it has become apparent that bimetallic units are also often uniquely suited to roles in catalysis.[2] The structural chemistry of metal dimers is diverse in the extreme, as shown in Scheme 1, from the unsupported multiply bonded species such as $[Re_2Cl_8]^{2-}$ [3] through to the triply-bridged species such as $[Re_2(\mu\text{-}Cl)_3Cl_6]^{1-}$.[4] In the unsupported cases, the dimer unit is dependent wholly on the metal-metal bond for its stability but in the bridged analogues, in contrast, metal-metal bonding is not essential, and indeed there are many examples such as $[Rh_2(\mu\text{-}Cl)_3Cl_6]^{3-}$ where it is entirely absent.[5] This has the important consequence that the cluster can adapt to changes in oxidation state without undergoing dissociation to monomeric fragments.

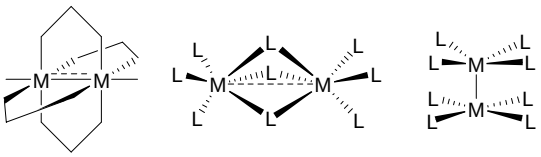

Scheme 1 Three structural categories of M_2^{n+} units.

The paddlewheel architecture (Scheme 1a) is exemplified by the Ru_2^{5+} compound $Ru_2(OAc)_4Cl$ that we use as the starting material here. Since the first report of this compound by Stephenson *et al*,[6] a large number of analogous di-ruthenium paddlewheel complexes in various oxidation states (Ru_2^{n+}, n = 4-7) have emerged in the literature.[7] These complexes are typically prepared by displacement of axial ligands such as Cl^- and/or the equatorial OAc^- ligand or, alternatively, *via* redox processes.[1, 8-12] In contrast, Ru_2^{n+} complexes with the face-shared bi-octahedral geometry (Scheme 1b) are relatively less common. The electronic demands placed on bridging ligands are very different in the paddlewheel and face-shared bi-octahedral motifs: the former requires bridging ligands that present two lone pairs that lie in the same plane, while single-atom bridges are ubiquitous in the face-shared species. These differences typically manifest themselves in very different geometries, with short Ru-Ru separations in the range 2.251-2.506 Å for the paddlewheels,[1,7] and much longer distances in the face-shared bi-octahedra (2.72-3.44 Å).[13,14,15,16] Thus, direct interconversion of the two structural types represents a significant challenge.

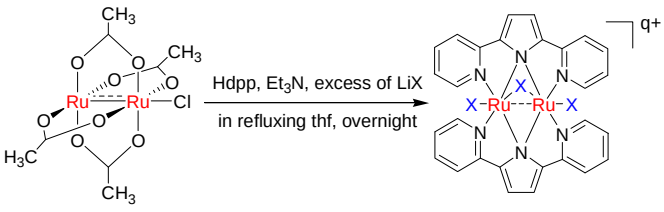

X = Br, q =0, (**1**); Cl, q =0, (**2**); I, q =1 (**3**)

Scheme 2 The synthesis of di-ruthenium complexes with dpp^- ligands.

[a] College of Chemistry and Chemical Engineering, Central South University, Changsha, Hunan 410083, China.
[b] A key Laboratory of Synthetic and Natural Function Molecule Chemistry of Ministry of Education, College of Chemistry and Materials Science, Northwest University, Xi'an 710127, P. R. China.
[c] Department of Chemistry, University of Oxford, South Parks Road, Oxford OX1 3QZ, UK.
[d] College of Pharmacy, University of Babylon, Hilla, Iraq
E-mail: xyyi@csu.edu.cn; liubin@nwu.edu.cn; john.mcgrady@chem.ox.ac.uk

†Electronic Supplementary Information (ESI) available: Details of experimental methods and additional data. CCDC 1943624. For ESI and crystallographic data in CIF or other electronic format see DOI: 10.1039/x0xx00000x

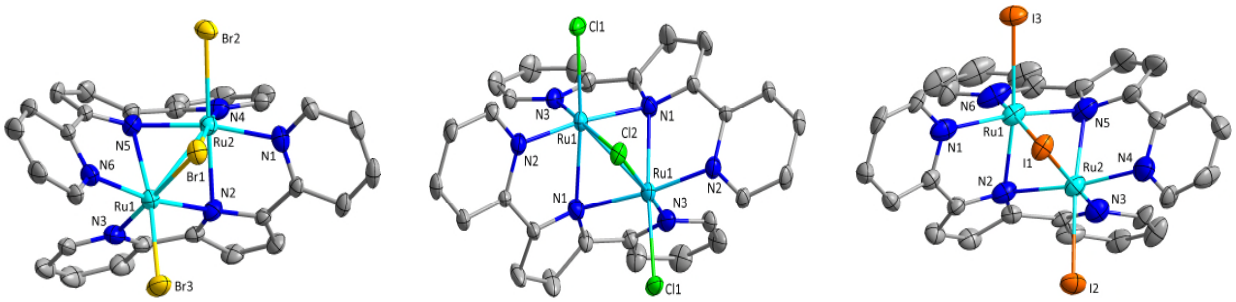

Figure 1 Solid-state structures of complexes **1**, **2** and **3**$^{+}$.

In previous work, we have reported the ability of 2,5-di(2-pyridyl)pyrrolide (abbreviated as Hdpp) to act as a bridging ligand between two Cu^{I} centres in [Cu$_2$(μ-κ$_2$N,N′:κ$_2$N′,N′′-dpp)(μ-X)(PPh$_3$)$_2$].[17] The dpp^{-} ligand binds to the two copper centres via the two terminal pyridyl groups as well as the central nitrogen of the pyrrole ring, which acts as a bridge. The close proximity of the copper atoms results in non-negligible interactions between the centres. The coordination chemistry of the dpp^{-} ligand offers an interesting contrast with the closely-related di-pyridylamide ligand (dpa^{-}), the use of which was pioneered by both Cotton and Peng.[18,19] The dpa^{-} ligand also features two terminal pyridyl groups, which are linked by a single amide group rather than a pyrrole ring. As a result of the monoatomic linker, the dpa^{-} ligands are less flexible than dpp^{-}, and tend to form tri-, rather than bi-metallic chains in an extension of the paddlewheel motif shown in Scheme 1. In this contribution we extend the coordination chemistry of the dpp^{-} ligand to ruthenium by synthesizing the mixed-valence clusters Ru$_2$(μ-κ$_2$N,N′:κ$_2$N′,N′′-dpp)$_2$(μ-X)(X)$_2$], X = Br and Cl along with the cationic iodide analogue, Ru$_2$(μ-κ$_2$N,N′:κ$_2$N′,N′′-dpp)$_2$(μ-I)(I)$_2$]$^{+}$. We also present a detailed study of the spectroscopic and magnetic properties of the bromide and draw comparisons to the known chemistry of other face-shared bi-octahedra.

In Scheme 2, we show that treatment of [Ru$_2$(OAc)$_4$Cl], Hdpp and Et$_3$N in the presence of excess freshly dried LiBr in refluxing thf affords the face-sharing bi-octahedral Ru$_2^{5+}$ di-ruthenium complex [Ru$_2$(μ-κ$_2$N,N′:κ$_2$N′,N′′-dpp)$_2$(μ-Br)(Br)$_2$] (**1**) in 26 % yield. Despite numerous efforts, we have been unable to improve on this yield, nor characterize the bi-products. A similar protocol using LiCl rather than LiBr yields the chloride analogue, [Ru$_2$(μ-κ$_2$N,N′:κ$_2$N′,N′′-dpp)$_2$(μ-Cl)(Cl)$_2$] (**2**). In contrast, using the iodide LiI results in the formation of the cationic cluster [Ru$_2$(μ-κ$_2$N,N′:κ$_2$N′,N′′-dpp)$_2$(μ-I)(I)$_2$]$^{+}$ (**3**$^{+}$) which crystallises along with a tri-iodide anion, I$_3^{-}$ and a single molecule of I$_2$ per cation (see SI). The ESI mass spectrum of **1** shows a strong peak due to the protonated molecular ion ([**1** + H]$^{+}$) at *m/z* 882.7695. Analysis of the IR spectrum over the course of the reaction shows the disappearance of the C=O resonance at 1400-1500 cm^{-1} in the starting material, [Ru$_2$(OAc)$_4$Cl], and also the N-H resonance of Hdpp at 3450 cm^{-1} : both observations indicate that a dpp^{-} ligand replaces OAc^{-}, and this is confirmed by the solid-state structure (*vide infra*). The NMR spectrum of **1** shows a number of broad peaks, consistent with its formulation as a mixed-valent species. The cyclic voltammograms of **1**, **2** and **3**$^{+}$ are compared in Figure S10. All three show a reversible redox wave (Ru$_2^{6+}$/Ru$_2^{5+}$) at ~0.30 V *vs* Ag/AgCl and an irreversible reduction (Ru$_2^{5+}$ to Ru$_2^{4+}$) at about –0.77 V vs Ag/AgCl. **3**$^{+}$ has a further quasi-reversible redox wave at +0.66 V due to the I$_2$/I^{-}and/or I$_3^{-}$/I^{-} couple. The relatively small separation between the oxidation and reduction waves (1.07 V) is typical of systems where the unpaired electron in the mixed-valence system is delocalized over both centres.[14] The very similar cyclic voltammetry for the three complexes suggests that the isolation of the iodide as a cation rather than a neutral species probably reflects the availability of the I$_3^{-}$ counter-anion rather than any fundamental difference in stability of the two oxidation states.

A solution of **1** in CH$_2$Cl$_2$ was layered in hexane to give fine darkish-brown single crystals which proved suitably for X-ray diffraction analysis. Complex **1** is *C*$_2$ symmetric and crystallises in a triclinic lattice with space group P2$_1$/c. The structure, shown in Figure 1, is based on a face-sharing bi-octahedral architecture, with the nitrogen atoms of the two central pyrrole rings acting as bridges, along with a single bromide ligand. The coordination sphere at each ruthenium centre is then completed by two terminal pyridines from the dpp^{-} ligand and a further bromide ligand. The dpp^{-} ligands both have a μ-κ$_2$N,N**′**:κ$_2$N**′**,N**′′**-coordination mode, and the coordination geometry inevitably leads to a π stacking arrangement with closest C-C contacts at ~3.30 Å. The gross structural features of **2** and **3**$^{+}$ are very similar to **1**, all three featuring the same μ-κ$_2$N,N′:κ$_2$N′,N′′ coordination mode for dpp^{-} along with a single bridging halide. The important bond lengths of the three clusters are compared in Table 1. The Ru1-Ru2 bond lengths in **1** and **2** are 2.5414(4) Å and 2.5450(10) Å, respectively, distinctly shorter than in typical triply-bridged Ru$_2^{5+}$ complexes such as [Ru$_2$(μ-Cl)$_3$(NH$_3$)$_6$]$^{2+}$ (2.753 Å),[14] Ru$_2$(μ-Cl)$_3$Cl$_2$(PBu$_3$)$_4$ (3.28 Å) and Ru$_2$(μ-Cl)$_3$Cl$_2$(PMe$_2$Ph)$_4$ (3.44 Å).[15,16] The distance is, in fact rather more similar to those found in quadruply-bridged species such as the [Ru$_2$(OAc)$_4$Cl] starting material (2.287(2) Å), where typical values lie between 2.251 and 2.506 Å.[1,7] The short Ru-Ru bonds in **1** and **2** are, at first glance, indicative of much rather stronger Ru-Ru bond than found in typical Ru$_2^{5+}$ complexes. The bond length in the Ru$_2^{6+}$ compound **3**$^{+}$ is marginally shorter, at 2.4988(15) Å. In comparing these values, it is difficult to separate the effects of changing ligand (I *vs* Cl/Br) and oxidation state (Ru$_2^{6+}$ vs Ru$_2^{5+}$). However, the geometries optimized using DFT, also shown in parenthesis in Table 1, offer an opportunity to compare all three complexes over both oxidation (full details are given in supporting information, Table S3)). Where comparison with experiment is possible, it is clear that the DFT calculations reproduce all of the important trends, and the optimized Ru-Ru bond lengths are within 0.03 Å of the experimental values in all cases. A like-for-like comparison then suggests that the identity of the halide has almost no influence on the Ru-Ru bond length in either oxidation state, while one-electron oxidation to the cation results in a small but systematic contraction of ~0.06 Å. This change is very much smaller than that observed in tri-halide bridged analogues. Combined with the absence of any systematic dependence on the identity of the halide, this suggests that the geometry of the Ru$_2$ unit is determined almost entirely by small bridging nitrogen atoms

Journal Name

COMMUNICATION

Table 1. Structural parameters of **1**-**3** and **1**$^{+}$-**3**$^{+}$. X-ray data are shown in bold, DFT-computed values in parenthesis.

	1 (X = Br)	**1**$^{+}$	**2 (X = Cl)**	**2**$^{+}$	**3 (X = I)**	**3**$^{+}$
Ru-Ru / Å	**2.5414(4)** (2.52)	(2.46)	**2.5450(10)** (2.51)	(2.45)	(2.53)	**2.4988(15)** (2.48)
Ru-X_b / Å	**2.5352(5), 2.5392(5)** (2.58)	(2.56)	**2.4257(12)** (2.44)	(2.42)	(2.76)	**2.6974(14), 2.6961(4)** (2.74)
Ru-X_t / Å	**2.4822(6), 2.4768(5)** (2.45)	(2.43)	**2.3467(10)** (2.31)	(2.28)	(2.63)	**2.6241(14), 2.6278(14)** (2.61)
Ru-N_b (*trans* X) / Å	**2.276(3), 2.284(3)** (2.35)	(2.21)	**2.231(3)** (2.34)	(2.20)	(2.39)	**2.195(11), 2.178(12)** (2.23)
Ru-N_b (*trans* N) / Å	**2.167(3), 2.167(3)** (2.15)	(2.15)	**2.210(3)** (2.16)	(2.15)	(2.14)	**2.096(14), 2.131(13)** (2.14)
Ru-N_t / Å	**2.023(3)-2.057(3)** (2.02)	(2.04)	**2.023(3), 2.037(3)** (2.02)	(2.03)	(2.03)	**2.042(12)-2.100(14)** (2.05)
Ru-X_b-Ru / °	**60.109(13)** (58.5)	(57.4)	**63.28(4)** (62.0)	(60.7)	(54.6)	**55.20(4)** (53.8)

which inevitably also lead to very contracted Ru-X_b-Ru angles. The bridging Ru-$N_{pyrrole}$ bond lengths are somewhat dependent on the trans ligand, with those *trans* to a halide ligand substantially longer than those *trans* to a pyridine group. The Ru-$N_{pyridine}$ bonds, in contrast, are short (2.023-2.057 Å) and much less dependent on the identity of the *trans* ligand.

The frontier Kohn-Sham orbital array in Figure 2 shows the characteristic features of the face-shared bi-octahedral architecture,[20,21] with doubly-occupied σ and singly-occupied Ru-Ru σ* orbitals, giving a net bond order of 0.5. The configuration is therefore qualitatively similar to other face-shared bi-octahedral Ru_2^{5+} compounds such as $[Ru_2(\mu\text{-}Cl)_3Cl_6]^{4-}$.[22] One-electron oxidation removes the electron in the σ* orbital, generating a closed-shell singlet state with a formal Ru-Ru bond order of 1.0 and the somewhat shorter bond lengths reported in Table 1.

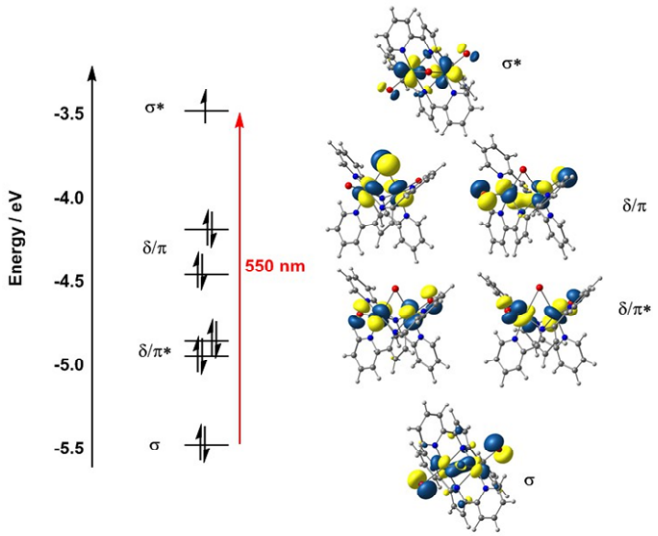

Figure 2 Frontier Kohn-Sham orbitals of **1**. Only the spin-β manifold is shown. The red arrow marks the σ→σ* transition.

The ground-state electronic structure offers a platform for interpreting the magnetic susceptibility of **1**, and also its EPR and UV/Visible spectroscopy. Powder EPR spectra collected at both 80 K and 250 K are identical (Figure 3A), and show a axial signal with g values of $g_x = g_y = 2.078$ and $g_z = 1.992$. For comparison, DFT-computed *g* values based on the ground-state electronic structure described in Figure 2 are $g_x = 2.051$, $g_y = 2.052$ and $g_z = 2.012$: the slight splitting of the g_x and g_y components reflects the inequivalence of the *x* and *y* axes in C_2 symmetry, but the splitting is clearly not large enough to be resolved in the experiment. An axial spectrum is typical of face-shared bi-octahedral Ru_2^{5+} systems, but the anisotropy is less pronounced than it is in $[Ru_2(\mu\text{-}Cl)_3(NH_3)_6]^{2+}$, for example, where $g_x = g_y = 2.100$ and $g_z = 1.950$.[20,23] The anisotropy of the *g* tensor can be traced to large off-diagonal elements of the spin-orbit operator between the δ/π and σ* orbitals shown in Figure 2, and the relatively low values of g_x and g_y in **1** are therefore consistent with a high-lying σ* orbital and hence strong Ru-Ru bonding. The plots of $\chi_M T$ and χ_M versus *T* for **1** in the temperature range of 1.8 - 300 K are shown in Figure 3B. The room temperature $\chi_M T$ value is 0.417 $cm^3\,K\,mol^{-1}$ (μ_{eff} = 1.826 μ_B), somewhat higher than the spin-only value for an $S = 1/2$ paramagnet (μ_{eff} = 1.732 μ_B). Upon cooling, $\chi_M T$ decrease slowly down to 20 K before dropping to a 0.219 $cm^3\,K\,mol^{-1}$ (μ_{eff} = 1.323 μ_B) at 1.8 K. Fitting the molar magnetic susceptibility to the Curie-Weiss law $\chi_M = C/(T-\theta)$, yields a Curie constant $C = 0.418\ cm^3 mol^{-1} K$ and $\theta = -2.84$ K: the negative θ value suggests the presence of weak antiferromagnetic interactions between neighbouring Ru_2^{5+} dimers in the crystalline lattice.

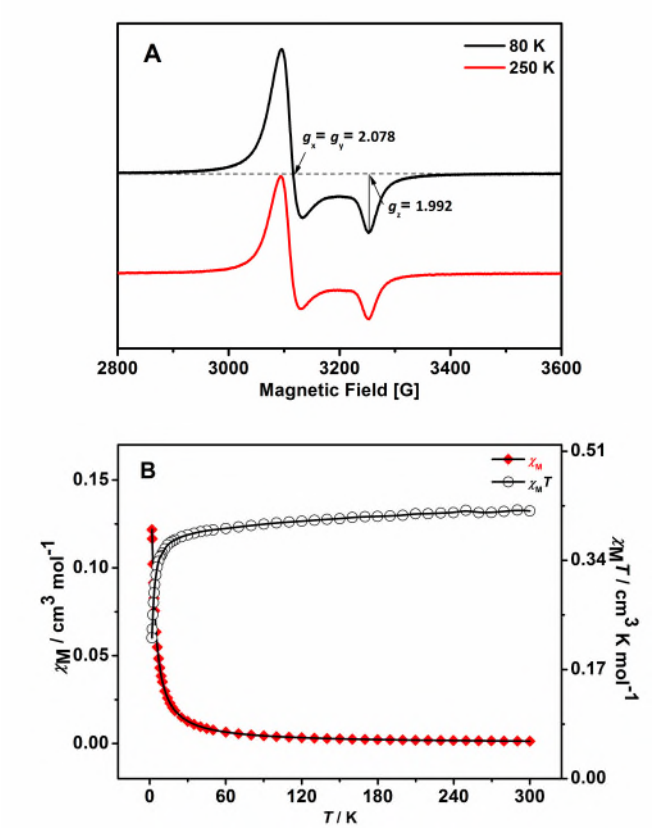

Figure 3 Magnetic properties of **1**: (A) Powder EPR spectra at 80 K and 250 K and (B) χ_M and χ_MT versus T.

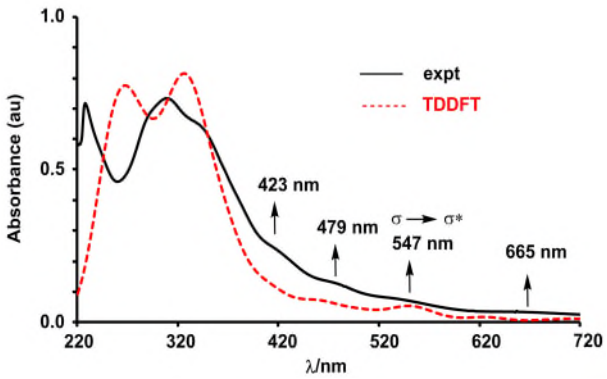

Figure 4 UV-vis spectrum of complex **1** (concentration of **1** is 2 μM) in CH_2Cl_2 and its TD-DFT computed spectrum.

The UV/Vis absorption spectrum of **1** shown in Figure 4 is strikingly different from that of the $Ru_2(OAc)_4Cl$ starting material (Figure S4), with absorption bands in region of 220-350 nm and 428 nm. The simulated spectrum calculated with time-dependent density functional theory (TD-DFT, BP86 functional), also shown in Figure 4 (red dashed line), reproduces the key features of the experimental data. The intense features below 400 nm have contributions from a large number of individual transitions, dominated by both intra-ligand π-π* transitions and Br→Ru charge transfer. In the closely-related tri-halide bridged "ruthenium blues" such as $[Ru_2(\mu\text{-}Cl)_3(NH_3)_6]^{2+}$ and $[Ru_2(\mu\text{-}Cl)_3Cl_6]^{4-}$, the strongly dipole-allowed σ→σ* transition is usually a prominent feature in the visible or near-IR region of the spectrum (typically above 800 nm).[20,22,23] The TD-DFT calculations on **1** show two moderately intense transitions around 550 nm, both with significant contributions from the σ→σ* one-electron excitation. There is no distinct feature in the spectrum in this region, but there is a shoulder at 547 nm on the rising edge of the charge transfer manifold that we tentatively assign to this transition. The substantial shift to shorter wavelengths compared to the tri-halide bridged blues is a result of the very short Ru-Ru bond, which imposes a greater splitting of the σ/σ* manifold.

In summary, we have reported here the synthesis, structure, electrochemistry and magnetism of a new family of face-shared bi-octahedral di-ruthenium complexes $Ru_2(\mu\text{-}\kappa_2N,N':\kappa_2N',N''\text{-}dpp)_2(\mu\text{-}X)(X)_2]^{q+}$. The structure contains a Ru_2 dimer unit, either with a Ru-Ru hemi-bond (bond order 0.5) for X = Cl and Br, q = 0, or a single bond (X = I, q = 1). The Ru-Ru bond length is short in all cases, and ~0.06 Å shorter for the cations than for the neutral complexes. The relative insensitivity of the bond lengths to either halide or oxidation state reflects the constraining effect of the small nitrogen bridges. The spectroscopic and magnetic properties of **1** are all consistent with a delocalized (Robin-Day class III) mixed-valence Ru_2^{5+} dimer, with a single unpaired electron delocalized over both metal centres in the σ* orbital.

Acknowledgements This work was supported by the National Natural Science Foundation of China (project 21571190 and 21673172). M.O acknowledges the HCED in Iraq for a scholarship.

Notes and references

1 (a) F. A. Cotton, C. A. Murillo and R. A. Walton. (2005), *Mutiple Bonds Between Metal Atoms*, New York: Spinger Science and Business Media, Inc. 377-430; (b) S. T. Liddle (2015), *Molecular Metal-Metal Bonds: Compounds, Synthesis, Properties*, Weinheim, Germany, Wiley-VCH. 225-278.

2 I. G. Powers and C. Uyeda, ACS Catal., 2017, **7**, 936-958.

3 F. A. Cotton and C. B. Harris, *Inorg. Chem*., 1965, **4**, 330-333.

4 G.A. Heath, J. E. McGrady, R. G. Raptis and A.C. Willis, *Inorg. Chem.*, 1996, 35, 6838-6843.

5 F. A. Cotton and D. A. Ucko, *Inorg. Chim. Acta* 1972, **6**, 161-172.

6 T. A. Stephenson and G. Wilkinson, *J. Inorg. Nucl. Chem.,* 1966, **28**, 2285-2291.

7 M. Cortijo, R. González-Prieto, S. Herrero, J. L. Priego and R. Jiméne-Aparicio, *Coord. Chem. Rev.*, 2019, **400**, 213040-213062.

8 G. M. Chiarella, F. A. Cotton, C. A. Murillo, K. Ventura, D. Villagrán and X. P. Wang, *J. Am. Chem. Soc*., 2014, **136**, 9580-9589..

9 S. Ngubane, K. M. Kadish, J. L. Bear, E. V. Caemelbecke, A. Thuriere and K. P. Ramirez, *Dalton Trans.,* 2013**, 42**, 3571-3580.

10 G. L. Xu, A. Cordova and T. Ren, *J. Cluster Science,* 2004, **15**, 413-424.

11 J. S Pap, J. L. Snyder, Paula M. B. Piccoli and J. F. Berry, *Inorg. Chem.,* 2009, **48**, 9846-9852.

12 P. Angaridis, F. A. Cotton, C. A. Murillo, D. Villagrán and X. P. Wang, *J. Am. Chem. Soc*., 2005, **127**, 5008-5009.

13 J. Darriet, *Rev. Chim. Miner*., 1981, **18**, 27.

14 M. N. Hughes, D. O'Reardon, R. K. Poole, M. B. Hursthouse and M. Thornton-Pett, *Polyhedron*, 1987, **6**, 1711-1713.

15 R. C. Torralba, F. A. Cotton, *Inorg. Chem.,* 1991, **30***,* 2196-2207.
16 (a) J. Bravo, J. Castro, S. García-Fontán, M. C. Rodríguez-Martínez and P. Rodríguez-Seoane, *Eur. J. Inorg. Chem.*, 2006, 3028-3040; (b) G. Cavigliasso, T. Lovell and R. Stranger, *Dalton Trans.*, 2006, 2017-2025.
17 Y. P. Wang, J. J. Xiao, X. H. Hu and X. Y. Yi, *Inorg. Chim. Acta,* 2015**, 435**, 125-130.
18 E.-C. Yang, M.-C. Cheng, M.-S. Tsai and S.-M. Peng, *J. Chem. Soc., Chem. Commun.,* 1994*,* 2377.
19 F. A. Cotton, L. M. Daniels and G. T. Jordan, IV, *Chem. Commun.*, 1997, 421.
20 B. D. Yeomans, D. G. Humphrey and G. A. Heath, *Dalton Trans.*, 1997, 4153-4166.
21 G.A. Heath and J. E. McGrady, *J Chem. Soc., Dalton Trans*., 1994, 3759-3767.
22 B. J. Kennedy, *Inorg. Chim. Acta,* 1991*,* **190***,* 265-269.
23 L. Dubicki and E. Krausz, *Inorg. Chem*., 1985, **24**, 4461-4465.